

Frequency-Domain Finite-Difference Acoustic Modeling with Free Surface Topography using Embedded Boundary Method

*Junlun Li, Yang Zhang, and M. Nafi Toksöz
Earth Resources Laboratory,
Department of Earth Atmospheric and Planetary Sciences
Massachusetts Institute of Technology*

Summary

In this paper, we present a method to model acoustic wave propagation in the frequency-domain in the presence of free surface topography using the embedded boundary method. The advantage of this method is to solve for the pressure field at each frequency on regular finite difference grids but with sub-cell resolution (up to 2nd order accuracy) for the irregular free surface. The topographic free surface condition is implemented in 2nd order accuracy, as in the regular domain so that global 2nd order accuracy is guaranteed. We use the level set method to obtain the projection points and normal directions corresponding to the ghost points in the scheme in the irregular domain. The computational cost for solving the modified sparse matrix for the pressure field increases very little compared to that for a flat surface. We have benchmarked our solver with a 2-D Gaussian hill model and simulated wave propagating in a modified Canadian foothills model. This solver can be used as the forward engine in the full waveform inversion, and we are working underway to perform full waveform inversions with real land survey data with considerable presence of surface topography.

Introduction

Full waveform inversion is often considered as the latest and greatest technique for the sub-surface imaging and velocity analysis. Many authors have made considerable contributions in this field (e.g., Tarantola, 1984; Pratt et al., 1998; Pratt, 1999; Shin and Min, 2006). Most of these investigations assume a flat surface, as waveform modeling in the presence of free surface topography is usually difficult for the finite difference method. Staircase discretization is often adopted as an approximation to the tilted free surface (Oprsal and Zahradnik, 1999; Ohminato and Chouet, 1997; Robertsson, 1996). However, this approximation generates artificial scattering unless the discretization length is small, e.g., 1/60 of the dominant wavelength (Bleibinhaus and Rondenay, 2009).

The finite difference method with conforming grid technique (Hestholm and Ruud, 1998; Zhang and Chen, 2006; Appelö and Petersson, 2009) can provide satisfactory results for waveform modeling with topographic free surface. The coordinate transformation is involved in the method. For easier implementation, the collocation scheme is used which usually causes numerical instability in time stepping. Therefore great effort is required to mitigate oscillations associated with the collocation scheme. In addition, the Jacobian matrix used for transforming the coordinates regionally or globally usually causes additional computational cost.

The finite element method (e.g., Min et al., 2003) is often used to solve the wave propagation with topographic free surface boundary. However, the mesh generation remains a challenging issue, and numerical dispersion analysis is much more complicated.

There has been growing interest in the embedded boundary method (EBM) or similar methods in recent years (e.g., Kreiss and Petersson, 2006; Lombard et al., 2008). These authors developed EBM schemes in the time-domain that are able to describe an interface cutting through a regular finite difference cell at an arbitrary angle. However, collocation grids are required for EBM, which usually generates oscillations in time stepping.

In this paper, we developed a frequency domain finite difference method to model acoustic wave propagation in media with a free surface topography. We find that EBM is ideal for the frequency-domain finite difference scheme, as there is no oscillation issue as observed in time-domain. Compared with the conforming grid technique, the EBM requires modification only on the grid points next to the boundary. Considering that a majority of full waveform inversion studies are performed in the frequency-domain, our method could be an ideal forward engine in waveform inversion. In the following sections, we first introduce the numerical implementation of our solver, then benchmark our solver with a 2D Gaussian hill model and present results for simulation of wave propagation in a 2D Canadian foothills model.

Frequency-Domain Method

This section is organized in the following order: 1) discretization in the regular domain; 2) implementation of the embedded boundary method in the irregular domain; 3) matrix modification for ghost points; and 4) level set method for projection point and normal direction. Here, the regular domain refers to the region where the finite difference stencil is not cut through by the free surface boundary, i.e., the interior region that is not in contact with the free surface; the irregular domain refers to the stencils cut through by the boundary, having at least one point across the boundary. An example is shown in Figure 1.

The acoustic wave equation in frequency-domain is written as:

$$B(x, \omega) p(x, \omega) = s(x, \omega) \quad (1)$$

where $B(x, \omega)$ is the impedance matrix at location x and frequency ω , $p(x, \omega)$ is the pressure field and $s(x, \omega)$ is the Fourier transform of the source term. Note this is a second order differential equation for p . For the regular domain, we use the standard 5-point finite difference scheme (Pratt and Worthington, 1990; Hustedt et al., 2004) to discretize equation (1) as:

$$\begin{aligned} \frac{-\omega^2}{K_{i,j}} = & \frac{1}{\xi_{xi} \Delta^2} \left[\frac{b_{i+1/2,j}}{\xi_{xi+1/2}} (p_{i+1,j} - p_{i,j}) - \frac{b_{i-1/2,j}}{\xi_{xi-1/2}} (p_{i,j} - p_{i-1,j}) \right] \\ & + \frac{1}{\xi_{zi} \Delta^2} \left[\frac{b_{i,j+1/2}}{\xi_{zj+1/2}} (p_{i,j+1} - p_{i,j}) - \frac{b_{i,j-1/2}}{\xi_{zj-1/2}} (p_{i,j} - p_{i,j-1}) \right] + s_{i,j} \end{aligned} \quad (2)$$

where $K_{i,j}$ is the bulk modulus at (i, j) , Δ is the grid size, $b_{i,j}$ is the buoyancy (inverse of density), ξ_{xi} and ξ_{zi} are attenuation functions for the perfectly matched layered (PML).

The topographic free surface requires additional treatment in the discretization scheme. For a flat free surface, the ghost point method is often used (e.g., Graves, 1996). However, for an uneven free surface the ghost point method generates significant artificial scatterings. To correctly characterize the topographic free surface, we use the embedded boundary method to describe the boundary that may cut through a regular finite difference cell at an arbitrary angle (Kreiss and Petersson, 2006), and adapt it from time-domain to frequency-domain. The scheme is illustrated in Figure 1. The green dot indicates the central point ($p_{i,j}$) of a 5-point finite difference stencil used as an example. Its northern (p_1) and western (p_2) neighboring points are across the free surface and defined as ghost points of the central point $p_{i,j}$ and need to be estimated from interior points. We take p_1 as an example to show how to estimate these ghost points. For the pressure condition on free surface boundary, we have

$$p|_{x=\Gamma} = 0 \quad (3)$$

Using a three-point Lagrangian interpolation, the projection point $p_{1\Gamma}$ of p_1 on free surface Γ can be estimated from those points along its local normal direction (Figure 1). The interpolant can be written as:

$$p_{1\Gamma} = \alpha_1 p_1 + \alpha_2 p_{1i} + \alpha_3 p_{1ii} = 0 \quad (4)$$

where

$$\alpha_j = \prod_{f=1, f \neq j}^3 \frac{l_\Gamma - l_f}{l_j - l_f} \quad (5)$$

where l_Γ is the distance from p_1 to the boundary and l_j is the distance from p_1 to p_{1i} , or p_{1i} to p_{1ii} . By solving equation (4) with the boundary condition in equation (3), p_1 can be estimated with 2nd order accuracy (Kreiss and Petersson, 2006). To estimate the values for p_{1i} and p_{1ii} , we also use Lagrangian interpolation in the horizontal direction as indicated in Figure 1.

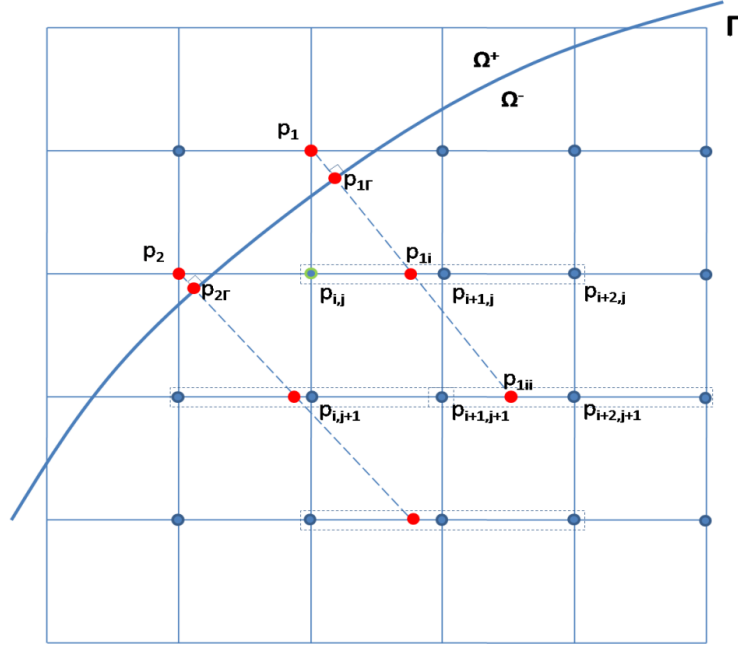


Figure 1. Illustration of the embedded boundary method. The green point ($p_{i,j}$) is the center point of a five-point stencil. Two of its ghost points (p_1, p_2) are across the free surface boundary and need to be estimated using interior points.

By the 2nd order interpolation in irregular domain, each ghost point now can be estimated by six interior points. For the stencils in the irregular domain, we need to modify the 5-point finite difference scheme by substituting for the ghost points the interior points. Take a 5-point stencil ($p_{i,j}, p_{i-1,j}, p_{i+1,j}, p_{i,j-1}, p_{i,j+1}$) with only one ghost point $p_{i,j-1}$ (northern) as an example, we have the modified finite difference scheme:

$$\begin{aligned}
\frac{-\omega^2}{K_{i,j}} = & \frac{1}{\xi_{xi}\Delta^2} \left[\frac{b_{i+1/2,j}}{\xi_{xi+1/2}} (p_{i+1,j} - p_{i,j}) - \frac{b_{i-1/2,j}}{\xi_{xi-1/2}} (p_{i,j} - p_{i-1,j}) \right] \\
& + \frac{1}{\xi_{zi}\Delta^2} \left[\frac{b_{i,j+1/2}}{\xi_{zj+1/2}} (p_{i,j+1} - p_{i,j}) - \frac{b_{i,j-1/2}}{\xi_{zj-1/2}} (p_{i,j}) \right. \\
& \quad - \frac{b_{i,j-1/2}}{\xi_{zj-1/2}} \left(\frac{l_2 m_1}{l_1} p_{i,j} + \frac{l_2 m_2}{l_1} p_{i+1,j} + \frac{l_2 m_3}{l_1} p_{i+2,j} \right. \\
& \quad \left. \left. + \frac{l_3 n_1}{l_1} p_{i,j+1} + \frac{l_3 n_2}{l_1} p_{i+1,j+1} + \frac{l_3 n_3}{l_1} p_{i+2,j+1} \right) \right] + s_{i,j}
\end{aligned} \tag{6}$$

where m, n are Lagrangian interpolation coefficients for p_{1i} and p_{1ii} , respectively. Compare equation (6) to equation (2), we see here $p_{i,j-1}$, i.e., the ghost point across the free surface has been substituted with six interior points ($p_{i,j}, p_{i+1,j}, p_{i+2,j}, p_{i,j+1}, p_{i+1,j+1}, p_{i+2,j+1}$).

To carry out the Lagrangian interpolation, we need to find the normal direction from the ghost point to the free surface and the corresponding projection length l_{Γ} . Instead of working on the parameterized 1D curve for free surface, we choose level set to represent the free surface as an interface between inner and outer domains, and related quantities.

Benchmarks

We use a 2D Gaussian hill as the free surface topography to validate our method. The “hill” is defined by the Gaussian function with a height of 100 m and standard deviation of 100 m. The top of the model is the free surface, and on the other three sides are PML boundaries. In simulation, a Ricker source wavelet with a central frequency of 10 Hz is excited at (1500, -1000) m. By inverse Fourier transforming the wave field solved in frequency-domain, we obtain the time-domain wave field shown in Figure 2. It can be clearly seen that, even a simple topographic free surface feature like the Gaussian hill generates a complicated reflection pattern.

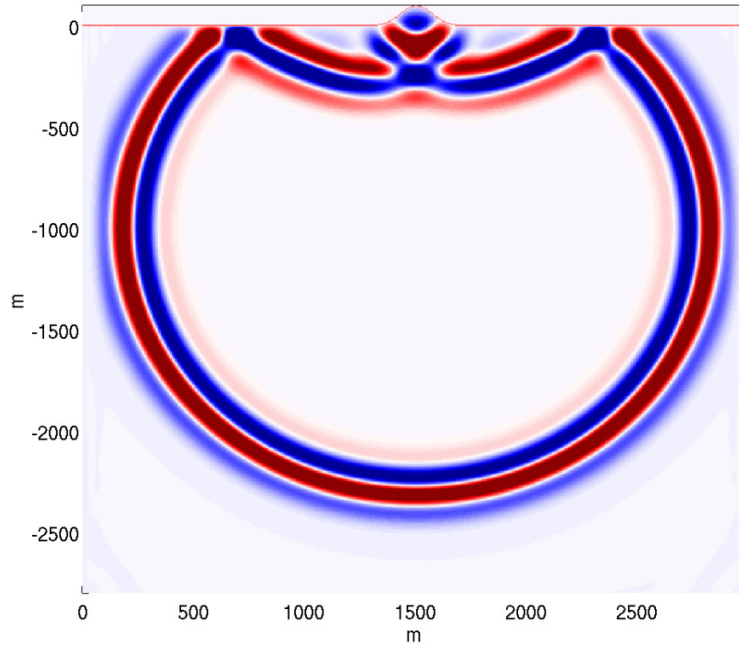


Figure 2. Snapshot of the wave field in a model with a Gaussian hill residing on top. The top of the model is a free surface, and the other three sides are PMLs.

We also benchmark our embedded boundary solver (EB) with a boundary conforming solver (BC) in time domain (Zhang and Chen, 2006). The BC solver has 4th order accuracy both in space and time, while our EB solver is 2nd order accuracy in space. In Figure 3, we compare the traces recorded at receiver placed at (1500, -700) m. We can see when we refine the grid spacing dx (from 10 m to 1.25m), the reflected waveforms computed from EB solver converge to the waveform from BC solver, which is taken as the most accurate result in this comparison.

We then study the convergence of our solver so as to validate it is 2^{nd} order accuracy globally. We use the result at $dx=1.25$ m as the reference, and calculate the L_2 and infinite norm of the “error” in reflected waveforms between the results with larger dx and the reference one. The convergence is plotted in a log-log scale in Figure 4, in which a 2^{nd} order convergence line is also plotted as a reference (black dashed line). From Figure 4, we can see that numerical results computed from our solver demonstrate a 2^{nd} order convergence both in L_2 and infinite norms, therefore we conclude that our solver has 2^{nd} order accuracy globally.

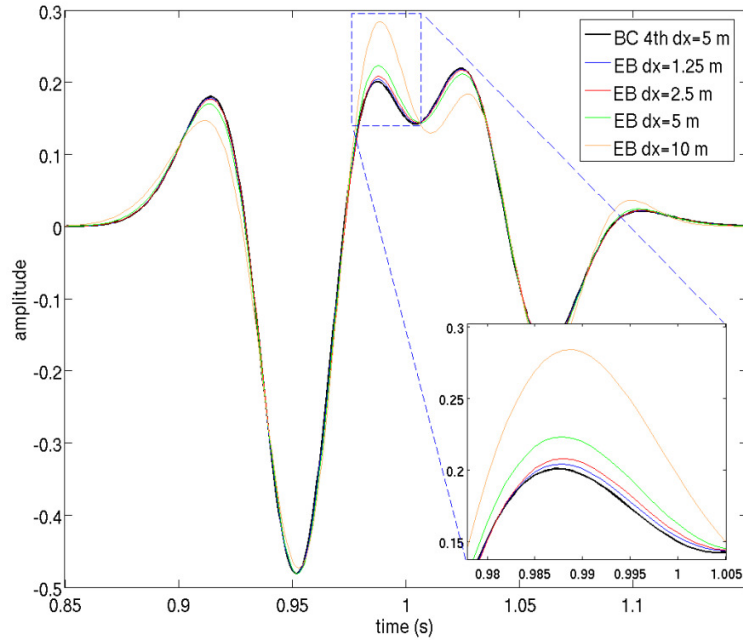


Figure 3. Comparison between Embedded Boundary (EB) method and Boundary Conforming (BC) method. Here EB is in frequency-domain and of 2^{nd} order accuracy, and BC is in time-domain and of 4^{th} order accuracy. Inset is an enlarged part of the waves in the dashed box.

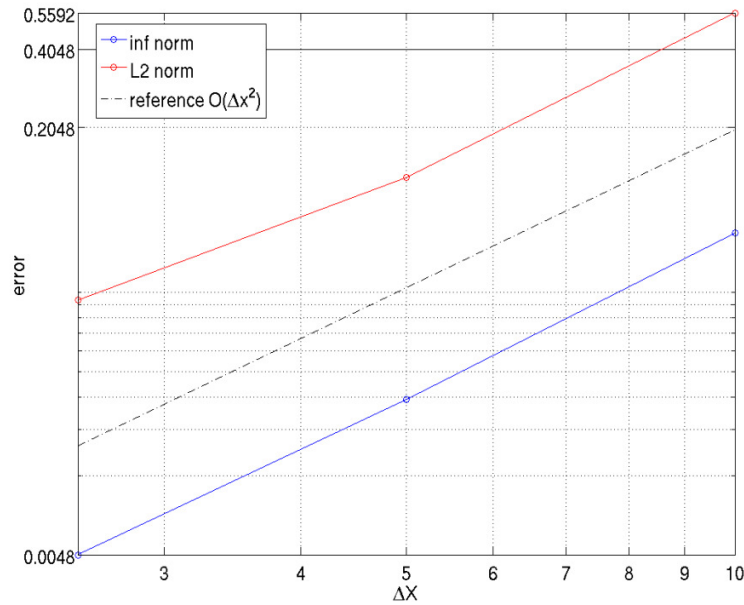


Figure 4. Convergence of the embedded boundary solver. A standard 2nd order convergence line (black dashed line) is plotted as a reference.

Examples

To demonstrate the capability of the EB solver on handling a more complicated case, we modeled wave propagating in Canadian foothills model shown in Figure 5. The velocity ranges from 3500 m/s to 6000 m/s. Complicated structures such as faults and domes are in the model. The surface elevation varies by amount of more than 1 km, and the whole model is discretized with 25 m grid spacing. Two cases in terms of different source locations are simulated. In the first case, the source is placed at $x=15.75$ km but on the surface, while in the second case we move the source down to -1.5 km. A Ricker source wavelet with a central frequency of 6 Hz is used. As shown in Figure 5 and 6, the wave field is complicated due to both the free surface topography and subsurface reflections. When the source is buried underground (Figure 6), we can clearly see how the reflected waves from free surface are distorted by the topography. Figure 7 shows the common shot gathers corresponding to these two cases, respectively.

Conclusions

In this study, we present a novel finite difference method to model the acoustic wave propagation in the frequency-domain in the presence of free surface topography with the embedded boundary method. The topographic free surface condition is implemented with 2nd order accuracy, as in the regular domain, such that global 2nd order accuracy is guaranteed. Although we used a standard 5-point stencil to discretize the wave equation in our study, the extension to the 9-point mixed-grid low dispersion stencil (Hustedt et al., 2004) should be straight forward, as the embedded boundary method can also be easily used in this discretization. We use the level set method to obtain the projection points and normal directions corresponding

to the ghost points in the scheme in irregular domain. The computation of surface normal directions and projections needs to be done only once, and its computational cost is negligible. The computation cost for solving the modified sparse matrix for the pressure field barely increases when compared to that of a flat surface case. We are working underway to apply our method in full waveform inversion for real field data with considerable surface topography.

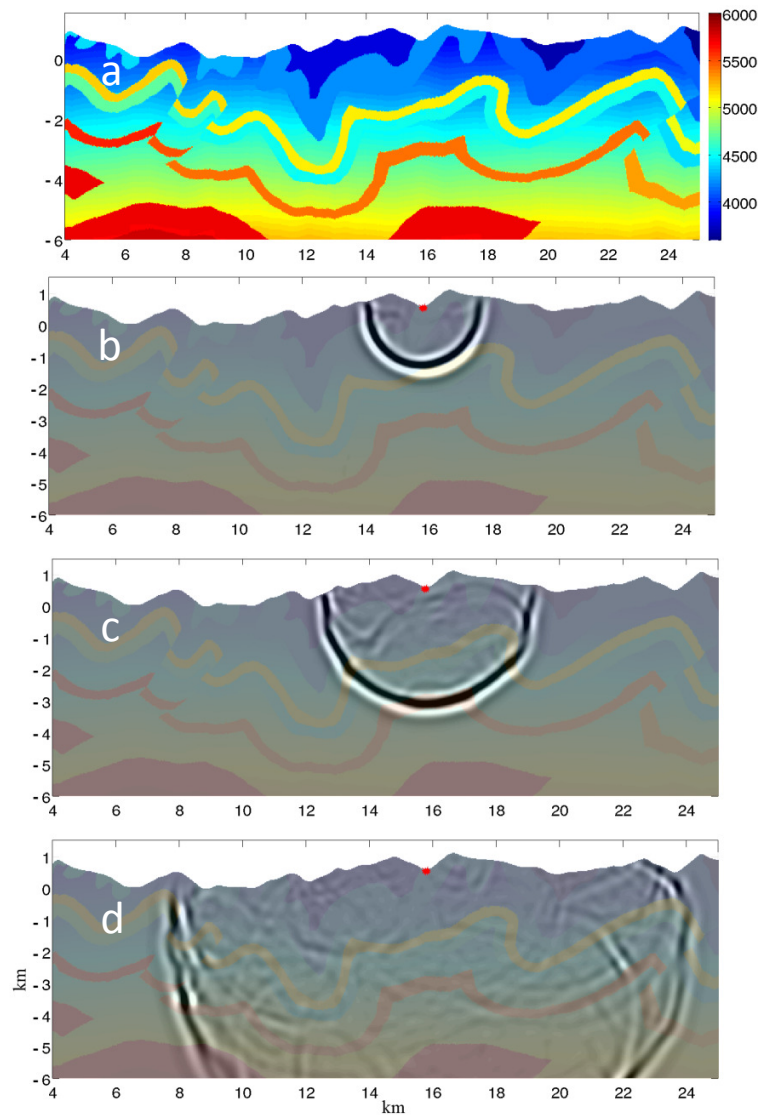


Figure 5. The Canadian foothills velocity model (a) and snapshots of the wave fields (b-d). The snapshots are taken at 0.78 s, 1.56 s and 2.34 s, respectively. The source is placed at $x=15.75$ km on the surface.

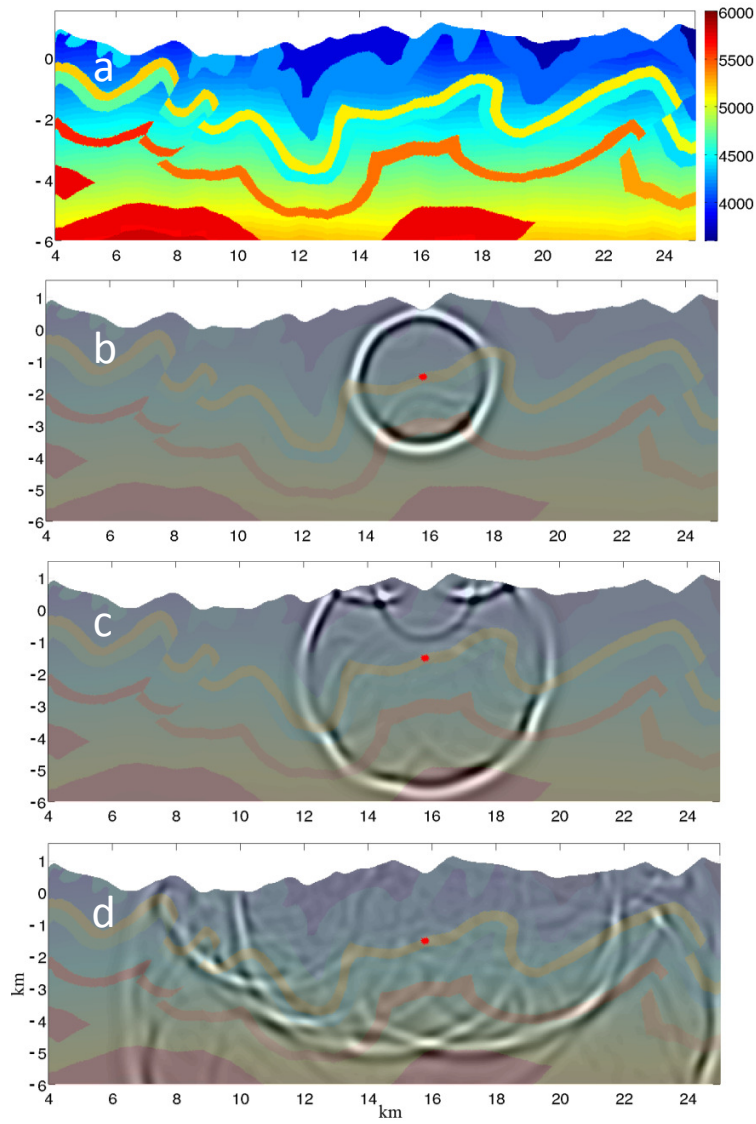


Figure 6. The Canadian foothills velocity model (a) and snapshots of the wave fields (b-d). The snapshots are taken at 0.78 s, 1.56 s and 2.34 s, respectively. The source is placed at (15.75 km, -1.5 km). The reflected waves from the free surface are clearly distorted by the topography.

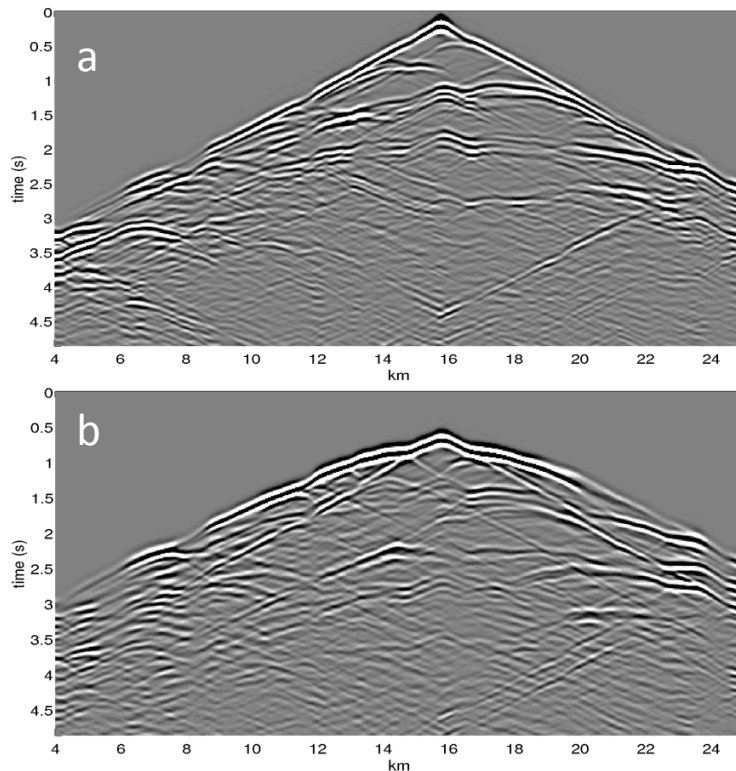


Figure 7. Common shot gathers calculated for the Canadian foothills model with source (a) at the surface and (b) buried at 1.5 km depth.

Acknowledgements

The authors want to thank Dr. Jie Zhang from GeoTomo for providing the foothills model. Also, the authors want to thank Dr. Wei Zhang for helpful discussions and providing the benchmark results.

References

- Appelö D. and N.A. Petersson, 2009, A stable finite difference method for the elastic wave equation on complex geometries with free surfaces, *Communication in Computational Physics*, **5**, 84-107.
- Bleibinhaus F. and S. Rondenay, 2009, Effects of surface scattering in full-waveform inversion, *Geophysics*, **74**, WCC69-WCC77.

- Graves R.W., 1996, Simulating seismic wave propagation in 3D elastic media using staggered-grid finite differences, *Bulletin of the Seismological Society of America*, **86**, 1091-1106.
- Hestholm, S. & B. Ruud, 1998, 3-D finite-difference elastic wave modeling including surface topography, *Geophysics*, **63**, 613–622
- Hustedt B. et al., 2004, Mixed-grid and staggered-grid finite-difference methods for frequency-domain acoustic wave modeling, *Geophysical Journal International*, **157**, 1269-1296.
- Kreiss H.O. and N.A. Pettersson, 2006, A second order accurate embedded boundary method for the wave equation with Dirichlet data, *SIAM Journal on Scientific Computing*, **27**, 1141-1167.
- Lombard B. et al., 2008, Free and smooth boundaries in 2-D finite-difference schemes for transient elastic waves, *Geophysical Journal International*, **172**, 252-261.
- Min, D.J. et al., 2003, Weighted-averaging finite-element method for 2D elastic wave equations in the frequency domain. *Bulletin of the Seismological Society of America*, **93**, 904-921.
- Ohminato, T. and B.A. Chouet, 1997, A free-surface boundary condition for including 3D topography in the finite-difference method, *Bulletin of the Seismological Society of America*, **87**, 494–515.
- Oprsal, I. and J. Zahradnik, 1999, Elastic finite-difference method for irregular grids, *Geophysics*, **64**, 240–250.
- Pratt, R.G. and M.H. Worthington, 1990, Inverse theory applied to multisource cross-hole tomography, part 1: Acoustic wave-equation method, *Geophysical Prospecting*, **38**, 287–310.
- Pratt R.G. et al., 1998, Gauss-Newton and full Newton methods in frequency-space seismic waveform inversion, *Geophysical Journal International*, **133**, 341-362.
- Pratt R.G., 1999. Seismic waveform inversion in the frequency domain, part 1: theory and verification in a physical scale model, *Geophysics*, **64**, 888-901.
- Robertsson, J., 1996, A numerical free-surface condition for elastic/viscoelastic finite-difference modeling in the presence of topography, *Geophysics*, **61**, 1921–1934.

Shin C. and D.J. Min, 2006, Waveform inversion using a logarithmic wavefield, *Geophysics*, **71**, R31-R42.

Tarantola, A., 1984, Inversion of seismic reflection data in the acoustic approximation: *Geophysics*, **49**, 1259–1266.

Zhang W. and X.F. Chen, 2006, Traction image method for irregular free surface boundaries in finite difference seismic wave simulation, *Geophysical Journal International*, **167**, 337-353.